

# FORMATION OF MASSIVE MOLECULAR CLOUD CORES BY A CLOUD-CLOUD COLLISION

TSUYOSHI INOUE<sup>1</sup> AND YASUO FUKUI<sup>2</sup>

*Draft version July 22, 2022*

## ABSTRACT

Recent observations of molecular clouds around rich massive star clusters including NGC3603, Westerlund 2 and M20 revealed that formation of massive stars can be triggered by a cloud-cloud collision. By using three-dimensional, isothermal, magnetohydrodynamics simulations with the effect of self-gravity, we show that massive, gravitationally unstable, molecular cloud cores are formed behind the strong shock waves induced by the cloud-cloud collision. We find that the massive molecular cloud cores have large effective Jeans mass owing to the enhancement of magnetic field strength by shock compression and turbulence in the compressed layer. Our results predict that massive molecular cloud cores formed by the cloud-cloud collision are filamentary with the typical thickness of 0.1 pc and are threaded by magnetic fields perpendicularly to the filament.

*Subject headings:* stars: formation — instabilities — magnetic fields — shock waves

## 1. INTRODUCTION

Massive stars are astronomically very interesting objects that affect surrounding medium by strong radiation and stellar wind, cause supernovae and probably gamma ray bursts in their end of life, and leave neutron stars and black holes. However, how massive stars are formed in molecular cloud is still a matter of debate (e.g., Zinnecker & Yorke 2007). It has been studied from the theoretical point of view that massive stars can be formed by gravitational collapse of massive molecular cloud cores (Nakano et al. 2000; McKee & Tan 2002; Yorke & Sonnhalter 2002; Krumholz et al. 2009) and/or by competitive gas accretion in stellar cluster forming region (Bonnell et al. 2004). These works mostly focused on massive star formation in a given gravitationally unstable core as an initial condition. Thus, in order to draw up a complete scenario of massive star formation, we need to clarify how massive gravitationally unstable objects are formed in a molecular cloud.

CO observations by NANTEN2 telescope have revealed two distinct molecular clouds in the star burst cluster NGC3603, which includes more than 30 O stars, and it has been shown that a cloud-cloud collision triggered the cluster formation in the shock compressed layer (Fukui et al. 2013, submitted to ApJ). NANTEN2 observations discovered two more cases of massive star formation by similar cloud-cloud collisions in Westerlund 2 (Furukawa et al, 2009; Ohama et al. 2010) and in M20 (Torii et al. 2011), suggesting the importance of such triggering in massive star formation. One of the most outstanding features of the massive star forming cloud-cloud collisions is that the typical relative speed of the collisions is as large as  $20 \text{ km s}^{-1}$  ( $\sim 100$  in sonic Mach number), while the colliding clouds have variety of mass and size.

The cloud-cloud collision was studied using hydrodynamics simulations by Habe & Ohta (1992) and Anathpindika (2010). They found that the cloud-cloud collision induces the formation of cloud cores by enhanced self-gravity as a consequence of shock compression. In the previous studies, the role of magnetic field on the core formation has been neglected. If we omit the magnetic field, the shock compression by the strong collision tend to generate cores with lower mass, since

density enhancement generally leads to smaller Jeans mass. However, if we take into account the effect of magnetic field, mass of the cores formed behind the shock can be enhanced owing to the strengthened magnetic field and enhanced effective Jeans mass. In this paper, by using three-dimensional, isothermal, magnetohydrodynamics (MHD) simulations with the effect of self-gravity, we examine the cloud-cloud collision and the formation of gravitationally unstable objects formed in the shock compressed layer.

## 2. SETUP OF SIMULATIONS

We solve the ideal MHD equations with the self-gravity, and assume the isothermal equation of state with the sound speed of  $c_s = 0.2 \text{ km s}^{-1}$ , which corresponds to the medium of temperature  $T = 12 \text{ K}$  and mean molar weight 2.4. The basic MHD equations are solved by using the second-order Godunov-type finite-volume scheme (van Leer 1979) that implements an approximate MHD Riemann solver developed by Sano et al. (1999). The consistent method of characteristics with the constrained transport technique is used for solving the induction equations (Clarke 1996). The integration of the ideal MHD part of the basic equations is done in the conservative fashion. The Poisson equation for the self-gravity is solved by using the multi-grid method (William et al. 1988) in which boundary condition is computed by the method developed by Miyama et al. (1987).

We prepare a cubic numerical domain of the side lengths  $L_{\text{box}} = 8.0 \text{ pc}$  that is composed of  $1024^3$  or  $512^3$  uniform numerical cells depending on the model (see Table 1), indicating that the physical resolution is  $\Delta x \simeq 0.008 \text{ pc}$  or  $0.016 \text{ pc}$ . Because molecular clouds are characterized by supersonic turbulence that induces density fluctuations, we initially set the isothermal gas with density fluctuations. The fluctuations are given as a superposition of sinusoidal functions with various wave numbers from  $2\pi/L_{\text{box}} \leq |k| \leq 80\pi/L_{\text{box}}$  and random phases. The power spectrum of the density fluctuations is set as an isotropic power law:  $(\log \rho)_k^2 k^2 \propto k^{-2}$ , which can be expected by supersonic turbulence that follows Larson's law (Beresnyak et al. 2005). Thus, our initial density structure is parameterized by mean density  $\langle n \rangle_0$  and dispersion  $\Delta n \equiv (\langle n^2 \rangle - \langle n \rangle_0^2)^{1/2}$ . The model parameters are summarized in Table 1.

In order to study the shocked layer generated by a cloud-cloud collision, we set the initial velocity  $v_x(x) = v_{\text{coll}} \tanh[(5 -$

<sup>1</sup> Department of Physics and Mathematics, Aoyama Gakuin University, Sagamihara, Kanagawa 252-5258, Japan; inouety@phys.aoyama.ac.jp

<sup>2</sup> Department of Physics, Graduate School of Science, Nagoya University, Furo-cho, Chikusa-ku, Nagoya 464-8602, Japan

TABLE 1  
 MODEL PARAMETERS

Model No.	1	2	3	4	5	6	7
$\langle n \rangle_0$ [ $\text{cm}^{-3}$ ]	300	300	300	1000	300	300	300
$\Delta n / \langle n \rangle_0$	0.33	0.33	0.33	0.33	0.33	0.33	0.50
$B_0$ [ $\mu\text{G}$ ]	20	20	20	20	10	20	20
$v_{\text{coll}}$ [ $\text{km/s}$ ]	10	10	10	10	10	5.0	10
Gravity	Yes	Yes	No	Yes	Yes	Yes	Yes
Resolution [pc]	8.0/1024	8.0/512	8.0/1024	8.0/512	8.0/512	8.0/512	8/512
$M_{\text{core,tot}}$ [ $M_{\text{sun}}$ ]	194	167	N/A	126	35	24	69
$M_{\text{mag}}$ [ $M_{\text{sun}}$ ]	122	124	N/A	63	14	36	34
$M_{\text{turb}}$ [ $M_{\text{sun}}$ ]	71	41	N/A	63	21	53	34
$\langle n \rangle_{\text{core}}$ [ $\text{cm}^{-3}$ ]	8.4e4	8.3e4	N/A	4.9e5	3.1e5	2.0e4	1.7e5
$\langle B \rangle_{\text{core}}$ [ $\mu\text{G}$ ]	2.8e2	2.8e2	N/A	6.3e2	2.9e2	1.8e2	2.9e2
$\Delta v_{\text{core}}$ [ $\text{km s}^{-1}$ ]	1.2	0.97	N/A	1.3	0.86	0.23	1.0
$t_{\text{form}}$ [Myr]	0.63	0.63	N/A	0.29	0.36	0.78	0.39

$10x)/L_{\text{box}}$ , i.e., two flows collide head on in the  $y$ - $z$  plane at the centre of the numerical domain with relative velocity of  $2v_{\text{coll}}$ . Because the shock waves induced by the collision are very strong, the resulting shocked layer is magnetized almost parallel to the shocked layer. Also, if the collision is accidental, the colliding clouds would have different orientation of magnetic fields. Thus, the initial magnetic field is set as  $\vec{B} = (0, B_0 \cos[\pi/4], B_0 \sin[\pi/4])$  for  $x \leq L_{\text{box}}/2$  and  $(0, B_0 \cos[\pi/4], B_0 \sin[-\pi/4])$  for  $x > L_{\text{box}}/2$ . We use the periodic boundary conditions for the  $x$ - $y$  and  $x$ - $z$  boundary planes, and we assume continuous colliding flows with periodic inhomogeneous density structure at the  $y$ - $z$  boundary planes.

It is widely known that artificial gravitational fragmentation can be avoided if the ratio of the Jeans length to the numerical resolution is larger than four (Trulove et al. 1997). As we show in the following, the effective Jeans length of the core is approximately 0.1 pc that is resolved approximately 13 cell lengths for Model 1 and 6.5 cell lengths for the other models.

### 3. RESULTS

#### 3.1. Fiducial model

The colliding streams induce two shock waves at  $x = L_{\text{box}}/2$  plane that propagate oppositely. In Model 1 (henceforth fiducial model), the sonic Mach number of the shock is approximately given by  $\mathcal{M}_s \simeq v_{\text{coll}}/c_s = 50$  and Alfvénic Mach number is  $\mathcal{M}_A \simeq v_{\text{coll}}/\langle c_A \rangle = 12.3$ . According to the shock jump condition for the isothermal MHD shock, the compression ratio is given by

$$r = \rho_1/\rho_0 = B_1/B_0 \simeq \sqrt{2}\mathcal{M}_A, \quad (1)$$

where subscript 0 (1) denotes preshock (postshock) state. Note that if we omit the effect of the magnetic field, the postshock density becomes  $r \simeq \mathcal{M}_s^2$  that is substantially different from the appropriate case of equation (1). This indicates that we cannot obtain reliable mass of a cloud core without the effect of magnetic field, since the larger density generally leads to smaller Jeans mass.

In the present simulations, upstream colliding clouds are inhomogeneous because molecular clouds are turbulent in general. When the shock wave hits a dense blob of the cloud, the shock surface is deformed due to the enhanced ram pressure. In Figure 1, we show the schematic of the gas stream in the postshock when the shock is deformed<sup>3</sup>: Because the deformed shock wave leads to a kink of stream lines across the

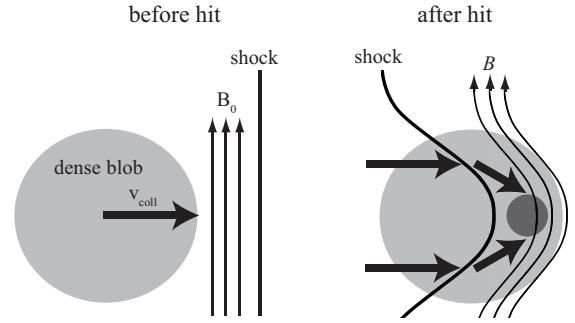


FIG. 1.— Schematics of the gas stream before (left) and after (right) the interaction between a shock and a dense blob. Because the deformed shock wave leads to a kink of stream lines across the shock, stream lines are headed toward convex point of the deformed shock wave.

shock, the stream lines are headed toward the convex point of the deformed shock wave. Owing to the effect of magnetic pressure, only the component of the kinked flows parallel to the postshock magnetic field lines can be converged and compressed that leads to the formation of a dense filament. Figure 2 shows the volume rendering map of the density (panel [a]) and column density structure of the shocked gas integrated along  $x$ -axis (panel [b] and [c]) at  $t = 0.63$  Myr since the impact. As expected, we can see the formation of dense filaments in the shocked layer even in the result of the simulation without self-gravity (see panel [c]). The black lines in panels (b) and (c) show the orientation of density weighted magnetic field projected onto the  $y$ - $z$  plane, indicating that the dense filaments are magnetized perpendicularly to the filaments as expected from the adobe theoretical expectation. Note that the integrations along  $x$ -axis for the column density and mean magnetic field are done only in the shocked layer.

In Model 3 (w/o self-gravity), the postshock density never exceed the value of  $n_{\text{cr}} \equiv 2 \langle n \rangle_0 (v_{\text{coll}}/c_s)^2$ , since the thermal pressure of the gas with  $n_{\text{cr}}$  is twice the mean ram pressure of the colliding clouds. In other words, it is a diagnostic of the formation of a gravitationally bound object (core), if the density exceed the critical value. In order to estimate the mass of the bound core, we employ the following sequence by using data when the local density exceeds the critical density: 1) Identifying connected region with the density larger than a threshold density  $n_{\text{thre}}$  that involves the density peak of  $n_{\text{cr}}$ . 2)

<sup>3</sup> One may find the abundance of previous works about the role of the interaction between a shock wave and upstream density fluctuations in the

astrophysics, e.g., Kornreich & Scalo (2000); Gicalone & Jokipii (2007); Kevlahan & Pudritz (2009); Inoue et al. (2009, 2012); Inoue & Inutuska (2012)

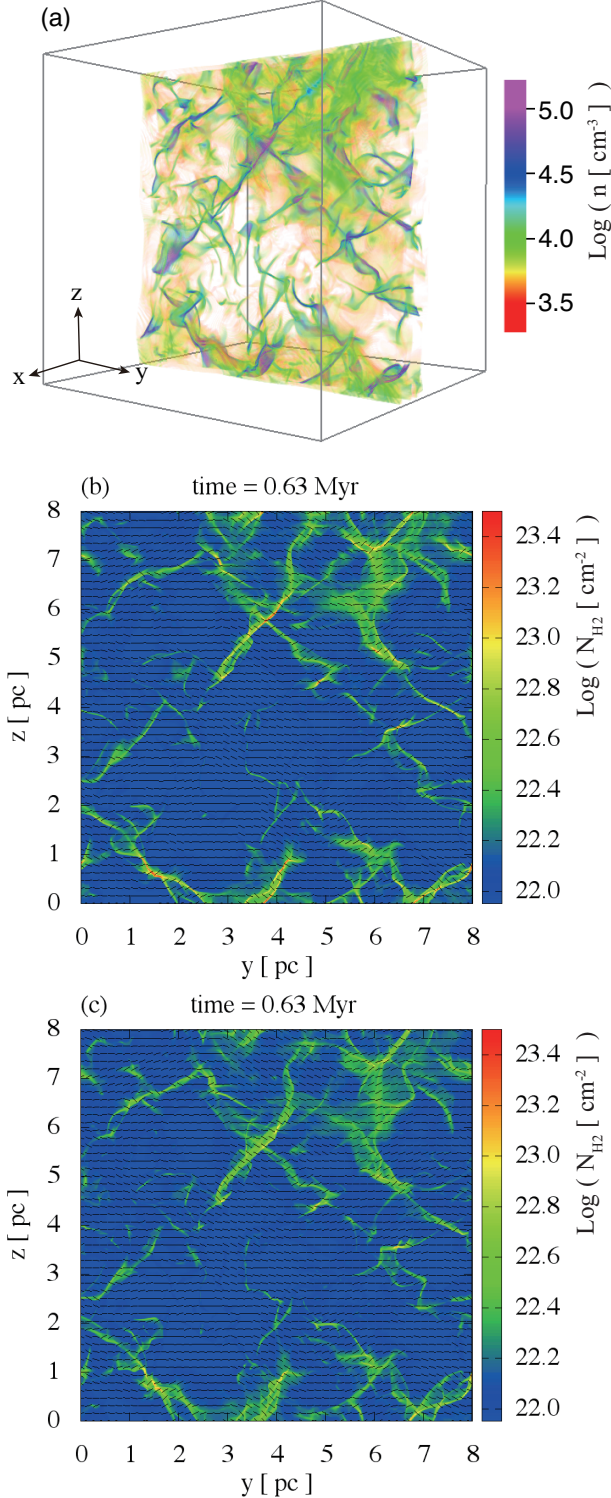


FIG. 2.— Panel (a): Volume rendering map of the density for Model 1 at  $t = 0.63$  Myr, in which the center of gravity of the massive core is located at  $(x, y, z) = (4.0, 6.1, 7.1)$  pc. Panel (b): Column density structure of the shocked gas integrated along  $x$ -axis for Model 1 at  $t = 0.63$  Myr since the impact. Panel (c): Same as panel (b) but for Model 3 (w/o gravity) at  $t = 0.63$  Myr. Black bars in panels (b) and (c) indicate the orientation of density weighted mean magnetic field along  $x$ -axis. Ranges of the color bars in panels (b) and (c) are set from 75% of the mean column density to  $23.5 \text{ cm}^{-2}$ . The integrations along  $x$ -axis for the column density and the magnetic field orientation are done only in the shocked layer.

Calculating the effective Jeans mass of the identified region:

$$M_{J,\text{eff}} \equiv \frac{\langle c_s \rangle^3 + \langle c_A \rangle^3 + \langle \Delta v \rangle^3}{G^{3/2} \langle \rho \rangle^{1/2}}, \quad (2)$$

where  $\Delta v$  is the velocity dispersion. 3) If the mass of the region  $M_{\text{core}}$  is smaller than  $M_{J,\text{eff}}$ ,  $n_{\text{thre}}$  is increased until  $M_{\text{core}}$  becomes identical to  $M_{J,\text{eff}}$ .

In the fiducial model, the massive core of  $M_{\text{core}} = 194 M_{\text{sun}}$  is formed at  $(x, y, z) = (4.0, 6.1, 7.1)$  pc and  $t = 0.63$  Myr. The average density of the core is  $\langle n \rangle = 8.4 \times 10^4 \text{ cm}^{-3}$  indicating that the thermal jeans mass of the core is  $M_{J,\text{therm}} = c_s^3 G^{-3/2} \langle \rho \rangle^{-1/2} = 0.40 M_{\text{sun}}$ . The ratios of Alfvénic and turbulent Jeans mass to the thermal Jeans mass are  $M_{J,\text{Alf}}/M_{J,\text{therm}} = \langle c_A \rangle^3 / \langle c_s \rangle^3 = 333$  and  $M_{J,\text{turb}}/M_{J,\text{therm}} = \langle \Delta v \rangle^3 / \langle c_s \rangle^3 = 196$ , respectively. Thus, the effective Jeans mass of the massive core is mainly enhanced by the strong magnetic field in the shocked layer (in the fiducial model, mean magnetic field strengths of the massive core and the shocked layer are  $|\langle \vec{B} \rangle_{\text{core}}| = 280 \mu\text{G}$  and  $|\langle \vec{B} \rangle_{\text{sh}}| = 178 \mu\text{G}$ , respectively).

### 3.2. Parameter dependency

In table 1, we summarize the physical parameters of the massive cores obtained by the results of the other models. Note that we focus only on the core that is formed at  $(x, y, z) = (4.1 \pm 0.3, 5.9 \pm 0.3, 7.2 \pm 0.3)$  where the massive core is also formed in Model 1. Thus, we can appropriately observe the effects of initial parameters on the core mass.

The lower resolution result (Model 2) shows that mass of the massive core is apparently smaller than that of the fiducial model. However, the difference is mostly attributed to the difference of the velocity dispersion (and consequently the turbulent Jeans mass) of the cores that is suppressed by numerical diffusion in the lower resolution run. The magnetic field strength and density of the core in Model 1 and Model 2 coincide well within 2% difference. This indicates that the Alfvénic Jeans mass is reliable even in the lower resolution simulations, while the turbulent Jeans mass can be underestimated.

The result of the fiducial model suggests that the mass of the massive core can be roughly estimated by the Alfvénic Jeans mass:  $M_{J,\text{eff}} \sim M_{J,\text{Alf}} \propto \langle B \rangle_{\text{core}}^3 / \langle \rho \rangle_{\text{core}}^2$ . If we substitute the mean density and magnetic field strength in the shocked layer given by eq. (1) for the above expression, we obtain  $M_{J,\text{Alf}} \propto B_0^2 v_{\text{coll}} \rho_0^{-3/2}$ . Since the density of the core is much larger than the mean density of the shocked layer due to the postshock converging flow (see Figure 1), above expression of the core mass is not clearly accurate. However, given that the mean magnetic field strength and mean density in the shocked layer correspond to the lower bounds of the core field strength and density, we can expect that the mass of the massive core is an increasing function of the initial magnetic field strength and the collision velocity, and that a decreasing function of the initial density. The results of Model 4 to Model 6 show that mass of the massive cores is  $126 M_{\text{sun}}$  for Model 4,  $35 M_{\text{sun}}$  for Model 5, and  $24 M_{\text{sun}}$  for Model 6 that are consistent with the above expectation.

The result of Model 7 (larger initial density fluctuations) shows the smaller core mass than the fiducial model. The reason for this can be explained quite reasonably: Because dense filament is formed by the postshock converging flows (see, Figure 1), density of the filament becomes larger as the amplitude of the shock deformation becomes larger. Thus, the stronger interaction between the shock and density fluctuation

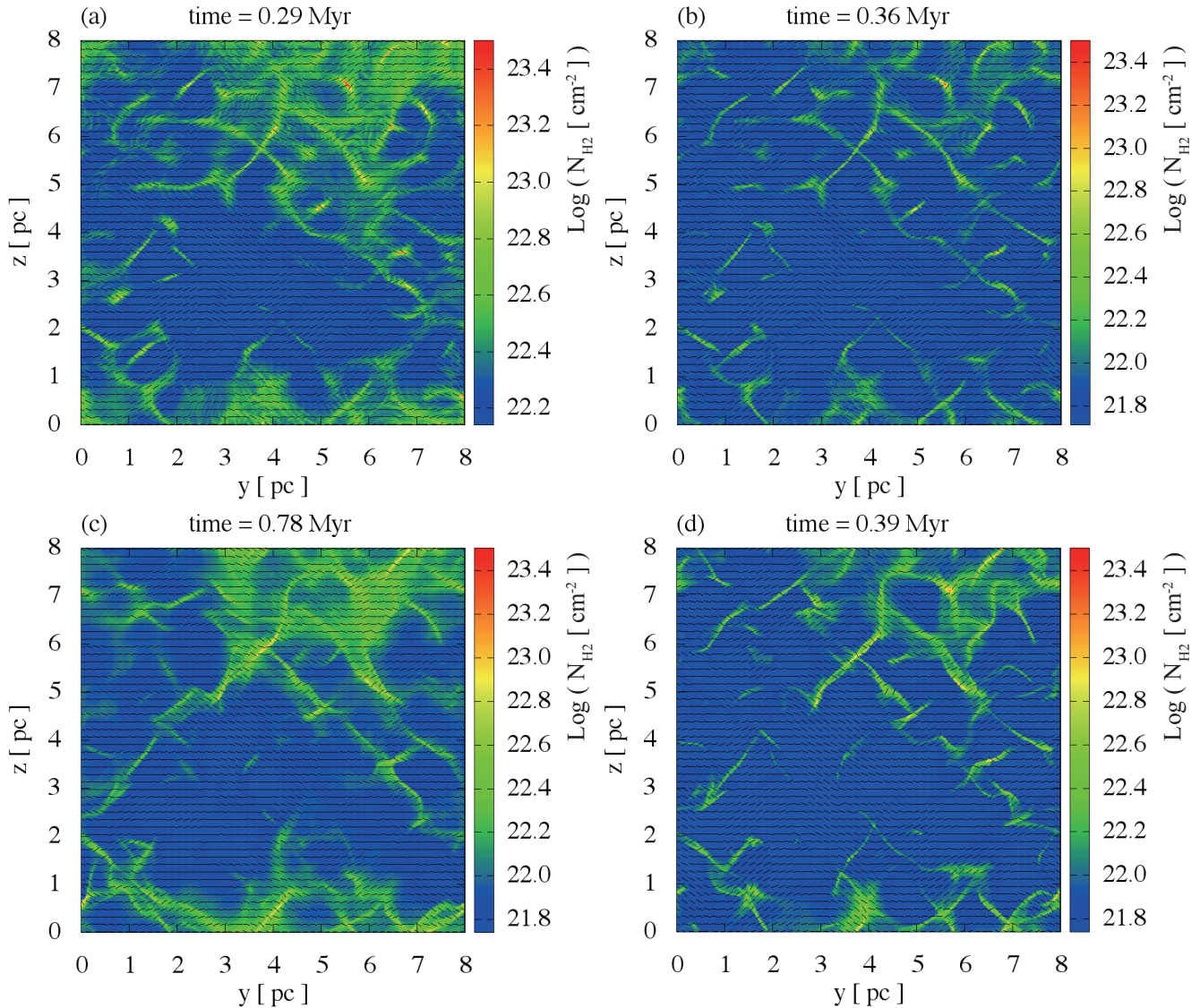


FIG. 3.— Panel (a): Column density structure of the shocked gas integrated along  $x$ -axis for Model 4. Panel (b)-(d): Same as panel (a) but for Models 5-7, respectively. Ranges of the color bars are set from 75% of the mean column density to  $23.5 \text{ cm}^{-3}$ . Black bars indicate the orientation of density weighted mean magnetic field along  $x$ -axis. The integrations along  $x$ -axis for the column density and mean magnetic field are done only in the shocked layer. All panels show snapshots of the time when the massive core is formed at  $(y, z) \sim (5.9, 7.2) \text{ pc}$ .

in Model 7 leads to higher filament density that results in a smaller core mass than the fiducial model.

The column density structures of Models 4-7 are shown in Figure 3. Interestingly enough, despite the different column density, the thickness of the dense filaments are surprisingly uniform with  $\simeq 0.1 \text{ pc}$  irrespective of the initial parameters. This invokes the recent discovery of  $0.1 \text{ pc}$  filaments in molecular clouds by Hershel space telescope (Arzoumanian et al. 2011). More detailed analysis about the distribution of the thickness will be presented in our subsequent paper.

#### 4. SUMMARY AND DISCUSSION

By using three-dimensional isothermal MHD simulations, we have studied the formation of massive molecular cloud core in the shocked layer induced by the intensive cloud-cloud collision. Our findings are as follows:

- The collision of inhomogeneous clouds generates dense filaments in the shocked layer. The direction of the magnetic field is perpendicular to the filaments, and the thickness of the filaments apparently takes uniform

value of  $\simeq 0.1 \text{ pc}$  irrespective of the initial parameters.

- The effective Jeans mass of the massive filament (core) is mostly determined by the Alfvénic and turbulent Jeans mass that is orders of magnitude larger than the thermal Jeans mass.
- The mass of the massive core is an increasing function of the initial magnetic field strength and collision velocity and a decreasing function of the initial density that can be simply understood from the shock jump conditions and the Alfvénic Jeans mass.

The formation of filaments indicates that a dense blob in the colliding cloud is compressed multi-dimensionally except perpendicular direction to the magnetic field by a single shock passage, because it is similar to an implosion process in a strongly magnetized medium. Such a multi-dimensional compression makes it possible to generate a high column density and high mass object.

In the present simulations, we stopped integration when the gravitationally bound massive core is formed. It is not

straightforward to conclude that massive stars are formed by the gravitational collapse of the massive core, because of the radiation feedback (Wolfire & Cassinelli 1987) and the fragmentation by turbulence (Dobbs et al. 2005). However, recent theoretical studies showed that massive stars can be formed by the gravitational collapse of a massive core, if column density of the core is larger than  $N_{\text{H}_2} \gtrsim 1 \text{ g cm}^{-2} \simeq 10^{23.4} \text{ cm}^{-2}$  owing to radiative heating (Krumholz & KcKee 2008) and/or if the massive core is strongly magnetized (Commercon et al. 2011; Myers et al. 2013). These studies strongly suggest that the massive cores induced by the cloud-cloud collision successfully forms massive star(s).

In this paper, we have focused only on massive core formation. However, the formation of dense filaments in the shocked layer can also be important in low-mass star formation. Recent MHD simulations that takes into account detailed atomic/molecular coolings and ultra-violet heating with appropriate shielding effects showed that molecular clouds are intrinsically clumpy, and clump-clump collision is the basic

process for the formation of gravitationally bound objects (Inoue & Inutsuka 2012). Thus, similar formation process of dense filaments is expected by the clump-clump collisions in a molecular cloud, suggesting that the 0.1 pc filaments discovered by Hershel telescope (André et al. 2010; Arzoumanian et al. 2011) are possibly generated by the mechanism found in this paper.

We thank S. Inutsuka, K. Omukai, and T. Hosokawa for helpful discussions. Numerical computations were carried out on XT4 and XC30 system at the Center for Computational Astrophysics (CfCA) of National Astronomical Observatory of Japan and K computer at the RIKEN Advanced Institute for Computational Science (No. hp120087). This work is supported by Grant-in-aids from the Ministry of Education, Culture, Sports, Science, and Technology (MEXT) of Japan, No. 23740154.

## REFERENCES

- Anathpindika, S. V. 2010, MNRAS, 405, 1431  
 André, P., et al. 2010, A&A, 518, L102  
 Arzoumanian, D., et al. 2011, A&A, 529, L6  
 Beresnyak, A., Lazarian, A., & Cho, J. 2005, ApJ, 624, L93  
 Bonnell, I. A., Vine, S. G., & Bete, M. R. 2004, MNRAS, 349, 735  
 Clarke, D. A. 1996, ApJ, 457, 291  
 Commercon, B., Hennebelle, P., & Henning, T. 2011, A&A, 530, 13  
 Dobbs, C. L., Bonnell, I. A., & Clark, P. C. 2005, MNRAS, 360, 2  
 Fukui, Y. et al. 2013, submitted to ApJ.  
 Furukawa, N. et al. 2009, ApJ, 696, 115  
 Habe, A. & Ohta, K. 1992, PASJ, 44, 203  
 Inoue, T., Yamazaki, R., & Inutsuka, S. 2009, ApJ, 695, 825  
 Inoue, T., Yamazaki, R., Inutsuka, S., & Fukui, Y. 2012, ApJ, 744, 71  
 Inoue, T., & Inutsuka, S. 2012, ApJ, 759, 35  
 Kevlahan, N., & Pudritz, R. E. 2009, ApJ, 702, 39  
 Kornreich, P., & Scalo, J. 2000, ApJ, 531, 366  
 Krumholz, M. R., & McKee, C. F. 2008, Nature, 451, 1082  
 Krumholz, M. R., et al. 2009, Science, 323, 754  
 McKee, C. F., & Tan, J. C. 2002, Nature, 416, 59  
 Miyama, S. M., Narita, S., & Hayashi, C. 1987, Prog. Theor. Phys., 78, 1273  
 Myers, A. T., et al. 2012, arXiv:1211.3467  
 Nakano, T., Hasegawa, T., Morino, J., & Yamashita, T. 2000, ApJ, 534, 976  
 Ohama, A. et al. 2010, ApJ, 709, 975  
 Sano, T., Inutsuka, S., & Miyama, S. M. 1999, Numer. Astrophys., 240, 383  
 Torii, K. et al. 2011, ApJ, 738, 46  
 Truelove, J. K. et al. 1997, ApJ, 489, 179  
 van Leer, B. 1979, J. Comput. Phys., 32, 101  
 William, H. P. et al. 1986, Numerical Recipes in Fortran77 (Cambridge University Press).  
 Wolfire, M. G., & Cassinelli, J. P. 1987, ApJ, 319, 850  
 Yorke, H. W., & Sonnhalter, C. 2002, ApJ, 569, 846  
 Zinnecker, H., Yorke, H. W. 2007, ARA&A, 45, 481